



## CHAPTER IV

### DEVELOPMENT OF POLYBENZOXAZINE MEMBRANES FOR ETHANOL ETHNOL–WATER SEPARATION VIA PERVAPORATION

#### 4.1 Abstract

Polybenzoxazine membranes have been successfully synthesized from bisphenol-A, formaldehyde, and three different types of diamines: hexamethylenediamine (hda), tetraethylenepentamine (tepa), and triethylenetetramine (teta) via a facile “quasi-solventless” method. To study the possibility of using polybenzoxazine membranes in a pervaporation system for ethanol-water separation, the sorption and swelling behaviors of these membranes were investigated. When hda was used as a reactant, the resulting polybenzoxazine membranes showed the best service time and interestingly only water permeated the membranes under the studied operation conditions. The total permeation flux was found to be  $1.52 \text{ kg/m}^2\text{h}$  and the separation factor was higher than 10,000. Additionally, an increased permeation flux was achieved by raising the temperature of the feed solution and decreasing the membrane thickness. The optimum conditions for this study were  $70 \text{ }^\circ\text{C}$  for the feed mixtures when a  $200 \text{ }\mu\text{m}$  thick was used.

**Keywords:** Pervaporation; Polybenzoxazine; Swelling; Sorption; Permeation flux; Separation factor

## 4.2 Introduction

Due to the substantial increase in the price of fuels and to global warming concerns, the development of alternative renewable energy has been a main research focus. One of these clean forms of renewable energy is biofuel—including biodiesel, bioethanol, biomethanol, biogas, etc. These fuels are produced from agricultural and industrial wastes with a very low prime cost. Fermentation is an attractive process for producing feedstock chemicals from renewable biomass. However, the low concentration of the fermentative products creates cost-intensive product separation.

Gasohol, which is a mixture of gasoline and ethanol, has higher octane number and better antiknock properties than gasoline. Furthermore, it not only burns slower and dissipates less heat, but its combustion process is also complete, resulting in reduced emissions of some pollutants [1]. Generally, the ethanol used in gasohol is derived from a distillation process that is the common ethanol–water separation technology used in the petrochemical industry [2]. Other techniques—such as liquid–liquid extraction, carbon absorption, air stripping, etc.—require high operating costs and, in some cases, have some limitations that make them unattractive for industrial applications [3]. The separation of alcohols from dilute aqueous solutions by distillation is unfavorable since the energy consumption required for purification exceeds the energy content of the alcohols recovered. To make the fermentation process economically attractive, a more efficient alcohol recovery process is preferred. The pervaporation (PV) technique is especially attractive for the separation of close-boiling-point liquids or azeotropes, e.g. an ethanol–water mixture, which cannot be separated by standard distillation processes. The PV technique utilizes the concept of partial vaporization of a liquid through a dense polymeric or ceramic membrane. The separation technique using polymer membranes has received much attention due to the design flexibility to improve the membrane selectivity and permeability [4–8].

Polybenzoxazine precursors have been synthesized from various aromatic/aliphatic amines, mono/diphenols, and formaldehyde [9–11]. One approach was to synthesize polybenzoxazine from a low molecular weight monomer, using monofunctional amine, phenol, and formaldehyde as reactants [10]. However,

polybenzoxazines obtained via this approach usually suffered from brittleness. Another method was the preparation of polybenzoxazine from high molecular weight oligomers from diamine, bisphenol-A, and formaldehyde [11]. The properties of the polybenzoxazines derived from these high molecular weight oligomers, especially brittleness, have been greatly improved when compared with cured films from the typical low molecular weight precursors. This enables polybenzoxazine to be an excellent candidate for flexible membrane applications [12–14]. In this study we have therefore illustrated how our polybenzoxazine membrane can be used to separate water from an ethanol–water mixture via the pervaporation technique.

### 4.3 Experimental

#### 4.3.1 Materials

Analytical grade 1,4-Dioxane was purchased from Labscan, Ireland. Bisphenol-A (BPA, 97% purity) and hexa-methylenediamine (hda, 98% purity) were purchased from Aldrich, Germany. Ethanol (99.9% purity) was purchased from J.T. Baker; White Group, Malaysia. Formaldehyde (analytical grade, 37%wt. in water) was purchased from Merck, Germany. Tetraethylenepentamine (tepa, 85% purity) and triethylenetetramine (teta, 85% purity) were purchased from Fluka, Switzerland. All chemicals were used as received.

#### 4.3.2 Measurements

The polybenzoxazine precursors were characterized by proton nuclear magnetic resonance spectroscopy ( $^1\text{H-NMR}$ , Varian Mercury 300) using deuterated chloroform ( $\text{CDCl}_3$ ) as the solvent. A differential scanning calorimeter (DSC7, PerkinElmer) was used to study the polymerization process by using a heating rate of  $10\text{ }^\circ\text{C}/\text{min}$  under a  $\text{N}_2$  flow. An attenuated total reflectance infrared spectrometer (ATR-IR, Thermo Nicolet Nexus 670) was used to determine the chemical structure using ZnSe  $45^\circ$  (flat plate) with a scanning resolution of  $4\text{ cm}^{-1}$ . The membrane morphology was investigated using a scanning electron microscope (SEM, JEOL model JSM-5410LV and Hitachi/s-4800). A thermogravimetric analyzer (TGA, PerkinElmer Pyris Diamond) was used to investigate the thermal stability of the

membranes using a heating rate of 20 °C/min under a N<sub>2</sub> flow. The tensile properties of the polybenzoxazine membranes were measured by using a universal testing machine (Lloyd/LRX) at a crosshead speed of 50 mm/min. The results of each sample were determined from an average of at least 10 tests.

### 4.3.3 Methodology

#### 4.3.3.1 *Synthesis of the Polybenzoxazine Precursors*

The polybenzoxazine precursors were prepared by mixing bisphenol-A, formaldehyde, and the diamines (hda, tepa, or teta) at a mole ratio of 1:1:4, respectively [15,16]. Firstly, bisphenol-A (6.84 g, 30 mmol) was dissolved in 1,4-dioxane (15 mL) in a 50 mL glass bottle and was stirred until a clear solution was obtained. A formaldehyde solution (9.73 g, 324 mmol) was then added to the bisphenol-A solution. The temperature was kept under 10 °C by using an ice bath. Diamine was then added dropwise into the mixture while continuously stirring for approximately 1 h until a transparent yellow viscous liquid was obtained [17]. When hda was used, heat treatment at 100 °C was required to accelerate the reaction, implying that the hda has lower reactivity than the tepa and the teta. The benzoxazine precursors were then purified by washing with a 0.1 M NaHCO<sub>3</sub> solution (200 mL) before solvent removal by evaporation and drying under vacuum. The purified benzoxazine precursors were then characterized using <sup>1</sup>H-NMR.

#### 4.3.3.2 *Preparation of the Polybenzoxazine Membranes*

The benzoxazine precursors were cast on glass plates at room temperature using an Elcometer 3580 casting knife film applicator (from the elcometer/inspection equipment). The membranes were dried at room temperature in air for one day, followed by drying at 80 °C in an air-circulating oven for 24 h to remove excess solvent.

### 4.3.4 Characterization of Sorption and Swelling Behaviors

The polybenzoxazine membranes (approximately 25 mm× 25 mm in size, 200 μm thick, and weighting about 0.1 g) were placed in the following solvents: ethanol, water, and various mixtures of ethanol and water (20, 40, 60, and 80% by volume of ethanol), for 8 h at room temperature to ensure the attainment of swelling

equilibrium. At the specific time, the membranes were removed from the mixtures and blotted with a tissue to remove excess liquid before being weighed and replaced in the mixtures. The procedure was repeated until a constant weight for each sample was obtained. The ATR-IR was used to investigate the sorption characteristics of the polybenzoxazine membranes. The degree of swelling,  $G_s$ , is defined by the following equation:

$$G_s = \frac{W_t - W_o}{W_o} \times 100\% \quad (4.1)$$

where  $W_t$  represents the weight of the swollen membrane and  $W_o$  is the initial weight of the membrane. The results obtained from each condition were the average of 4 to 6 tested membrane samples.

#### 4.3.5 Pervaporation Studies

A schematic of the pervaporation experiment is shown in Figure 4.1. The membrane was placed in a stainless steel module. A flow rate of 900 mL/min was used to circulate the mixture from the feed reservoir containing a 1:9 ethanol to water ratio to a permeation cell. The performance of the membranes were determined by measuring % ethanol in the permeate side to calculate the permeate water flux ( $\text{kg}/\text{m}^2\text{h}$ ) and the separation factor. The quantities of ethanol and water were determined using a gas chromatograph (GC, Agilent GC-6890). The samples (0.5  $\mu\text{L}$ ) were injected under the following conditions: the carrier gas was helium and the pressure was set at 55 kPa for the thermal conductivity detector (TCD). The isothermal oven temperature was set at 200 °C, while the injector and detector temperatures were set at 200 °C and 250 °C, respectively. The permeate flux and the separation factor were determined as follows:

##### 4.3.5.1 Permeation flux ( $J$ , $\text{kg}/\text{m}^2\text{h}$ )

The permeation flux ( $J$ ) was calculated from Eq. (4.2):

$$J = M/(At) \quad (4.2)$$

where

$M$  = permeate weight (kg),

$A$  = effective membrane surface area ( $\text{m}^2$ ), and

$T$  = pervaporation time (h).

#### 4.3.5.2 Separation factor ( $\alpha_{\text{water-ethanol}}$ )

The separation factor ( $\alpha_{\text{water-ethanol}}$ ) was calculated from Eq.

(4.3):

$$\alpha_{\text{water-ethanol}} = (Y_{\text{water}}/Y_{\text{ethanol}})/(X_{\text{water}}/X_{\text{ethanol}}) \quad , \quad (4.3)$$

where

$Y_{\text{water}}$  = the mole fraction of water in the permeate,

$Y_{\text{ethanol}}$  = the mole fraction of ethanol in the permeate,

$X_{\text{water}}$  = the mole fraction of water in the the feed, and

$X_{\text{ethanol}}$  = the mole fraction of ethanol in the feed.

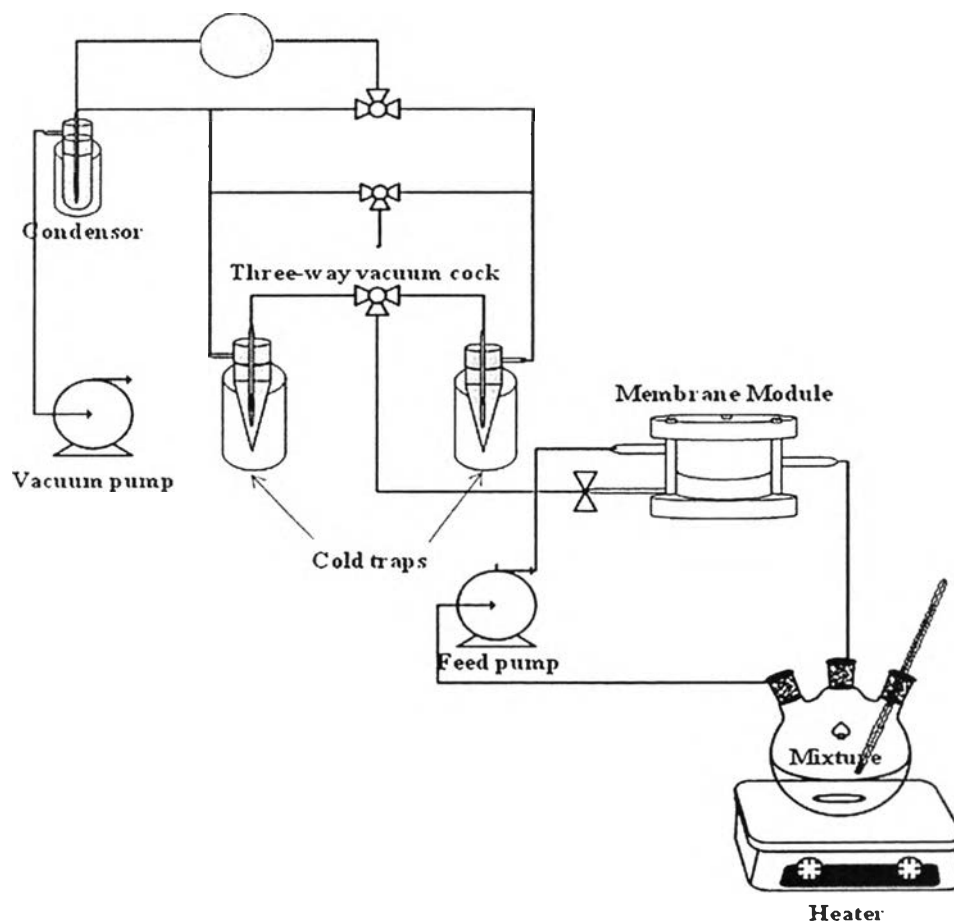


**Figure 4.1** Experimental set up for the pervaporation apparatus.

## 4.4 Results and Discussion

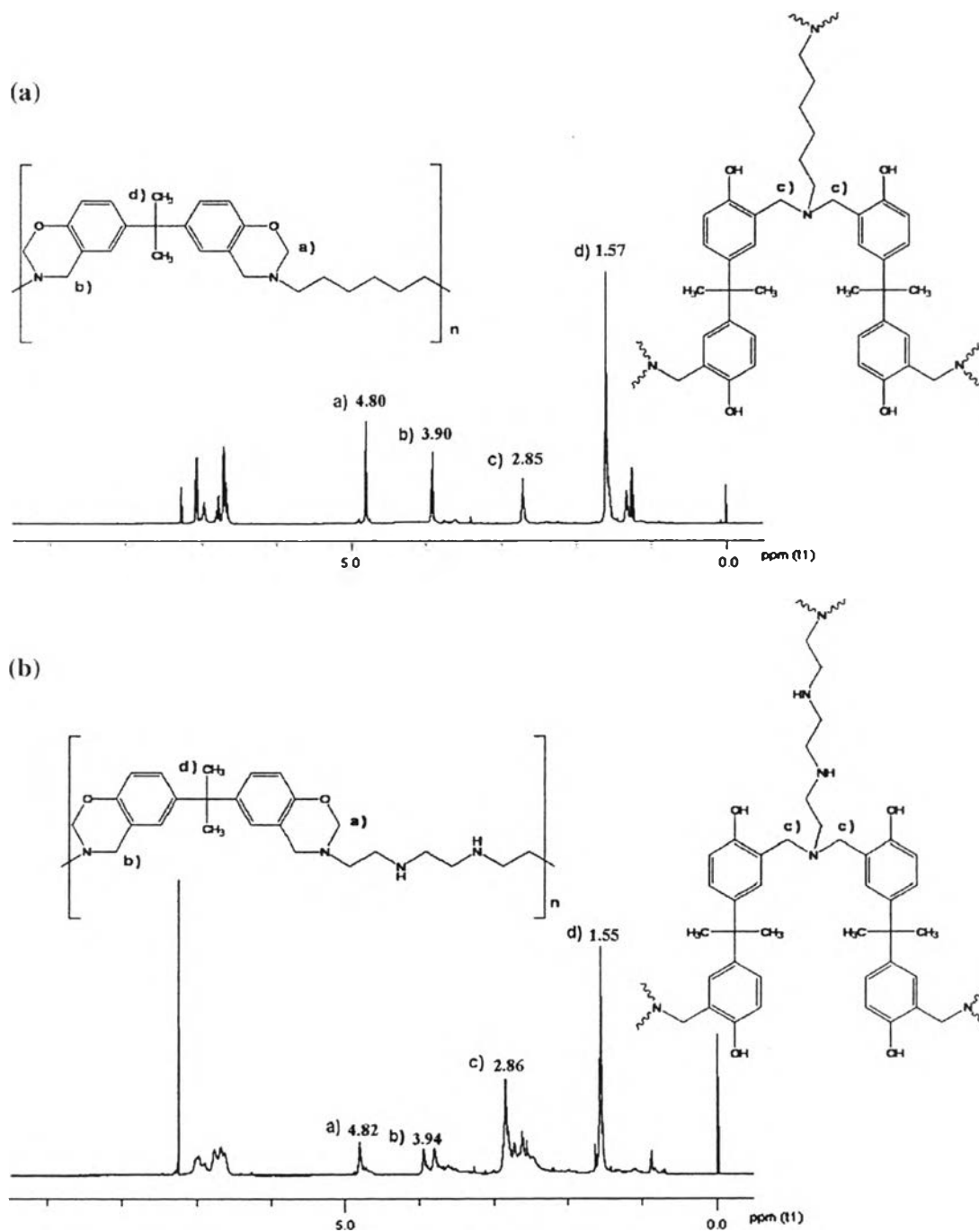
### 4.4.1 Characterization of Benzoxazine Precursors and Membranes

Benzoxazine precursors—abbreviated as poly(BA-hda), poly(BA-teta), and poly(BA-tepa)—were derived from the reaction of the diamines, the bisphenol-A, and the formaldehyde at a molar ratio of 1:1:4 via a quasi-solventless approach in which a small amount of dioxane was used only to facilitate the mixing of the reactants. The reaction took place within 1 h at low temperature, unlike the traditional solvent method, which requires much more solvent and a longer reaction time [10].

The  $^1\text{H-NMR}$  measurements were conducted to confirm the synthesis process (Figure 4.2). All of the precursors—poly(BA-hda), poly (BA-teta) and poly(BA-tepa)—derived from the different diamines showed the characteristic peaks assigned to the methylene protons of  $\text{O-CH}_2\text{-N}$  and  $\text{Ar-CH}_2\text{-N}$  of the ring-closed benzoxazine ring at approximately 4.80 to 4.82 and 3.90 to 3.94 ppm, respectively. The methyl protons of bisphenol-A were observed at 1.55 to 1.57 ppm. The methylene protons of the ring-opened benzoxazine were observed at 2.85 ppm. These results, especially for the poly(BA-hda), strongly agree with the results reported by Takeichi et al. [9,10], who also found the characteristic peaks corresponding to methylene protons of  $\text{O-CH}_2\text{-N}$  and  $\text{Ar-CH}_2\text{-N}$  in the ring-closed benzoxazine structure, at 4.86 and 3.97 ppm, respectively, the methylene protons of the ring-opened benzoxazine of  $\text{Ar-CH}_2\text{-N}$  at 2.85 ppm, and the methyl protons of bisphenol-A at 1.58 ppm.

The chemical structure of the prepared polybenzoxazine membranes were also confirmed using ATR-IR. The band of N-H stretching of the tetra and tepe was observed at around  $3400\text{ cm}^{-1}$ . The band at  $1502\text{ cm}^{-1}$  represents the stretching of the tri-substituted benzene ring. The out-of-plane bending vibration of C-H was observed at  $932\text{ cm}^{-1}$ . In addition, bands assigned to the asymmetric stretching of C-O-C and C-N-C were found at  $1233$  and  $1128\text{ cm}^{-1}$ , respectively. Furthermore, the  $\text{CH}_2$  wagging of the oxazine ring was also observed at  $1378\text{ cm}^{-1}$ . These FTIR results are in agreement with the study of Ning and Ishida [9], who also observed the asymmetric stretching of C-O-C ( $1234\text{ cm}^{-1}$ ), the asymmetric stretching of C-N-C

(1180 to 1187  $\text{cm}^{-1}$ ), the  $\text{CH}_2$  wagging of oxazine (1325 to 1328  $\text{cm}^{-1}$ ), the tri-substituted benzene ring (1502 to 1511  $\text{cm}^{-1}$ ), and the out-of-plane bending vibrations of C–H (1502 to 1511  $\text{cm}^{-1}$  and 937 to 943  $\text{cm}^{-1}$ ).





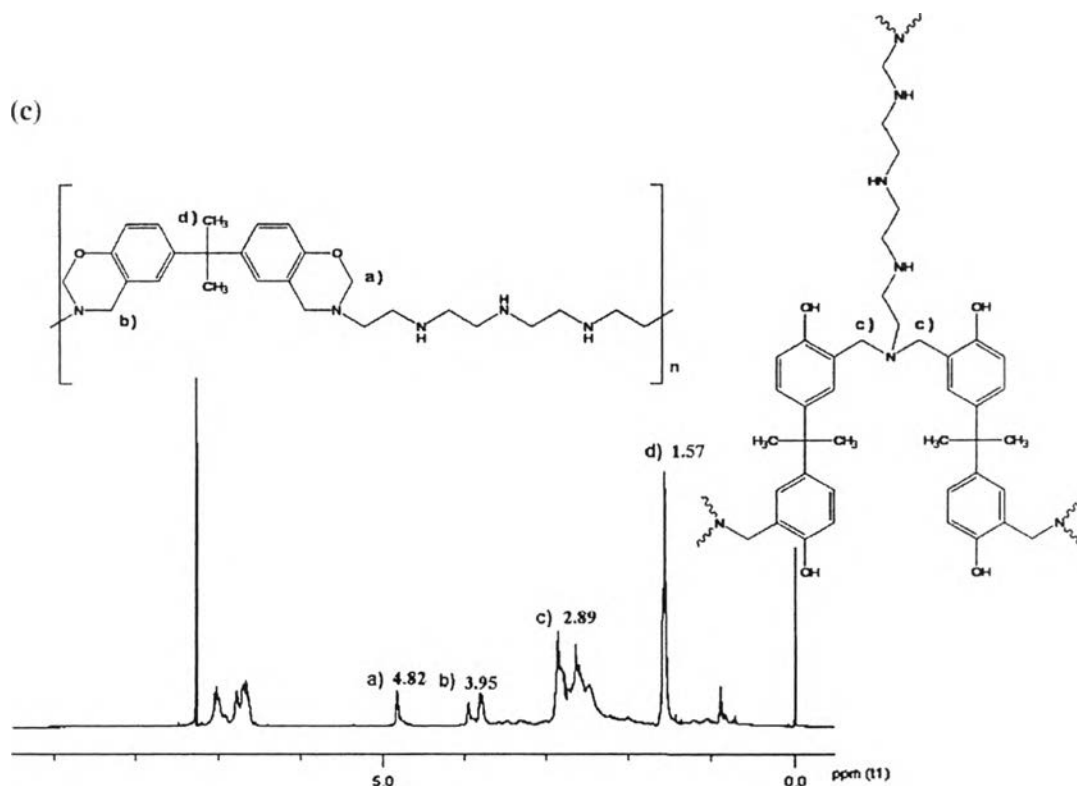


**Figure 4.2**  $^1\text{H-NMR}$  spectra of polybenzoxazine precursors: poly(BA-hda) (a), poly(BA-teta) (b), and poly(BA-tepa) (c).

The progress of the ring-opening polymerization of the poly-benzoxazine membranes was monitored by DSC (Figure 4.3). The DSC thermogram of partially-cured poly(BA-hda) shows an exothermic peak starting from 169 °C with a maximum at 248 °C, attributed to the benzoxazine ring-opening polymerization. After the precursor was fully cured, the exothermic peak disappeared. Similar results were found by Agag and Takeichi [11], who reported the onset of the exotherm of poly(BA-hda) at 171 °C with a maximum at 244 °C. Expectedly, when compared with the poly(BA-hda), the poly(BA-tepa) and poly(BA-teta), (having more nitrogen atoms in the molecules and stronger H-bonding) needed a greater amount of energy for the ring opening polymerization, leading to the shift of the exothermic peak to higher temperatures.

**Table 4.1** Thermal stability of the polybenzoxazine membranes

Membranes	T <sub>d</sub> -5% (°C)	T <sub>d</sub> -10% (°C)	% Char yield
Poly(BA-hda)	295	313	23
Poly(BA-teta)	269	285	21
Poly(BA-tepa)	269	281	20

The thermal stability of the polybenzoxazine membranes was investigated using TGA (Table 4.1); the polybenzoxazine membranes obtained from all three prepolymers showed thermal stability up to 240 °C. The TGA result of the poly(BA-hda) membrane is in agreement with the study of Takeichi and Agag [17], who reported that poly(BA-hda) began to degrade at around 240 °C, and the char yield was around 25%. The char yield of our membranes was in the following order: poly(BA-hda) > poly(BA-teta) > poly(BA-tepa). The poly(BA-tepa) showed the lowest char yield due to its high aliphatic content, leading to lower thermal stability. The stability of the membranes is important for applications that require a high operating temperature. However, in this pervaporation study, the appropriate temperature was only 70 °C.

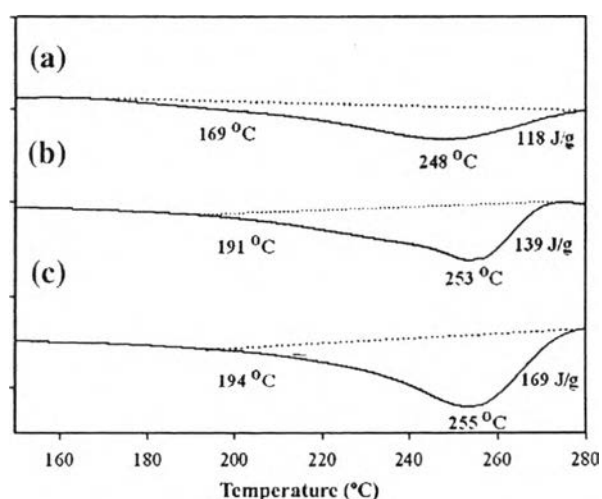


**Figure 4.3** DSC thermograms of polybenzoxazine membranes: poly(BA-hda) (a), poly(BA-teta) (b), and poly(BA-tepa) (c).

SEM micrographs show that the prepared polybenzoxazine membranes were dense and without any voids (Figure 4.4); Figure 4.4d–f clearly show that the prepared membranes were flexible and tough. Additionally, the mechanical properties were studied with tensile testing. (The tensile modulus, tensile strength, and elongation at break values are summarized in Table 4.2.) All three types of polybenzoxazine membranes showed similar modulus ( $E$ ). The tensile strength ( $\sigma_b$ ) and elongation at break ( $\epsilon_b$ ) of the polybenzoxazine membrane prepared from the high molecular weight precursors—Poly(BA-hda), Poly(BA-teta), and Poly(BA-tepa)—were higher than that of PB-a, which is a polybenzoxazine derived from a low molecular weight monomer. A higher elongation at break indicates greater flexibility. The tensile testing results of the poly(BA-hda) membrane were in agreement with those reported by Takeichi and co-workers, who studied the synthesis and thermal curing of high molecular weight polybenzoxazine precursors and the properties of the thermosets [10].

**Table 4.2** Tensile properties of the polybenzoxazine membranes

Membranes	$E$ (GPa)	$\sigma_b$ (MPa)	$\epsilon_b$ (%)	References
PB-a	3.3	37	1.6	[18]
PB-mda	3.5	87	4.1	[18]
PB-eda	3.3	58	2.4	[18]
PB-hda	2.0	65	4.1	[18]
Poly(BA-hda)	$1.78 \pm 0.14$	$42.58 \pm 6.03$	$3.96 \pm 0.67$	This study
Poly(BA-teta)	$1.77 \pm 0.22$	$50.76 \pm 6.84$	$5.04 \pm 2.00$	This study
Poly(BA-tepa)	$1.79 \pm 0.17$	$54.67 \pm 11.63$	$6.79 \pm 0.66$	This study

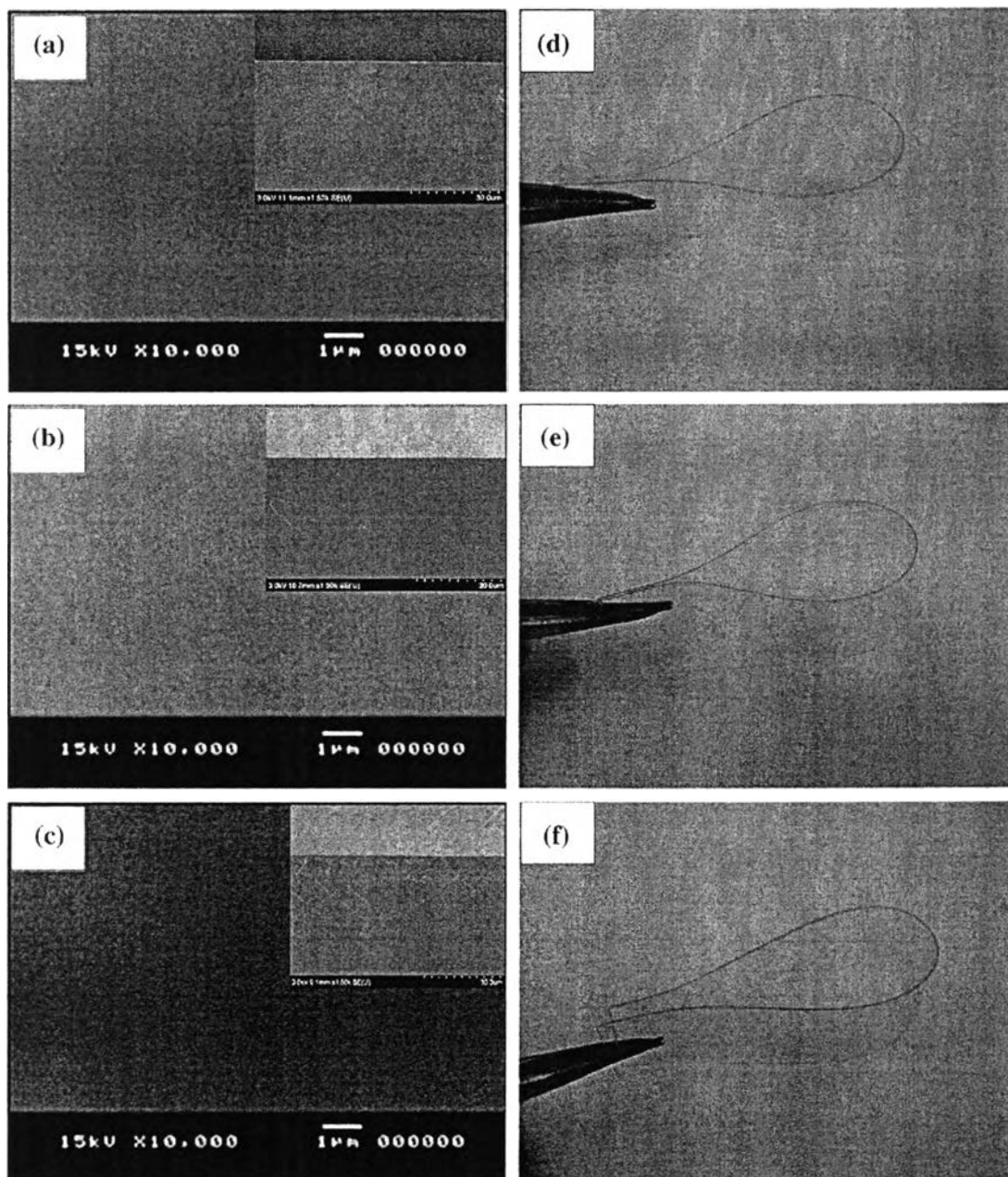


**Figure 4.4** SEM micrographs of surface, cross-section and appearances of poly(BA-hda) (a and d), poly(BA-teta) (b and e), and poly(BA-tepa) (c and f).

#### 4.4.2 Sorption and Swelling Behaviors of the Polybenzoxazine Membranes

Since the polarity of water (polarity index=9.0) is higher than that of ethanol (polarity index=5.2), the sorption behaviors of the polybenzoxazine membranes, corresponding to the ethanol and the water, must be different. The

polybenzoxazine molecular structure also affected the sorption and swelling activities [18]. Since the molecular structure of poly(BA-teta) and poly(BA-tepa) consisted of nitrogen atoms from the aliphatic diamine chains, these membranes could form hydrogen bonding with water. Thus, the longer the length of the aliphatic diamine, the more pronounced the effect on the sorption behavior of the polybenzoxazine and water. As clearly seen in the case of poly(BA-teta), the length of the aliphatic diamine chain is shorter; as a result, the degree of swelling was less than that of the poly(BA-tepa). On the other hand, the aliphatic diamine used to prepare poly(BA-hda) consisted of only aliphatic hydrocarbon; therefore, when ethanol was used as a media, the poly(BA-hda) membrane preferred to absorb ethanol since poly(BA-hda) is more hydrophobic when compared to poly(BA-teta) and poly(BA-tepa), leading to an increase in the degree of swelling. The poly(BA-tepa) membrane showed the highest degree of swelling in water (Figure 4.5a) due to the H-bondings between the nitrogen atoms in the aliphatic chain of the tepa and water molecules. As expected, the membranes derived from the poly(BA-hda) showed the lowest degree of swelling in water (Figure 5a) because there were no nitrogen atoms to form hydrogen bonds with the water molecules [19]. On the other hand, the swelling degree of poly(BA-hda) in ethanol was the highest (Figure 4.5b and c) since the aliphatic chains of the hda preferred to adsorb ethanol. A similar swelling behavior was observed by Chuang *et al.* [20], who studied the swelling activity by the sorption behavior of a hydrophobic membrane in water–ethanol mixtures. They found that the changes in the polymer swelling were due to the changes in the polymer's hydrophobicity.

Therefore, for ethanol–water separation, the sorption and swelling behaviors of polybenzoxazine membranes depend on the ratios of ethanol to water. The degree of swelling of the poly(BA-tepa) and the poly(BA-teta) membranes was increased when 60% by volume ethanol was used as a feed mixture because the polymer chains consist of both nitrogen atoms in the aliphatic chains and hydroxyl groups from the ring-opening polymerization, thus causing these membranes to swell in both ethanol and water.

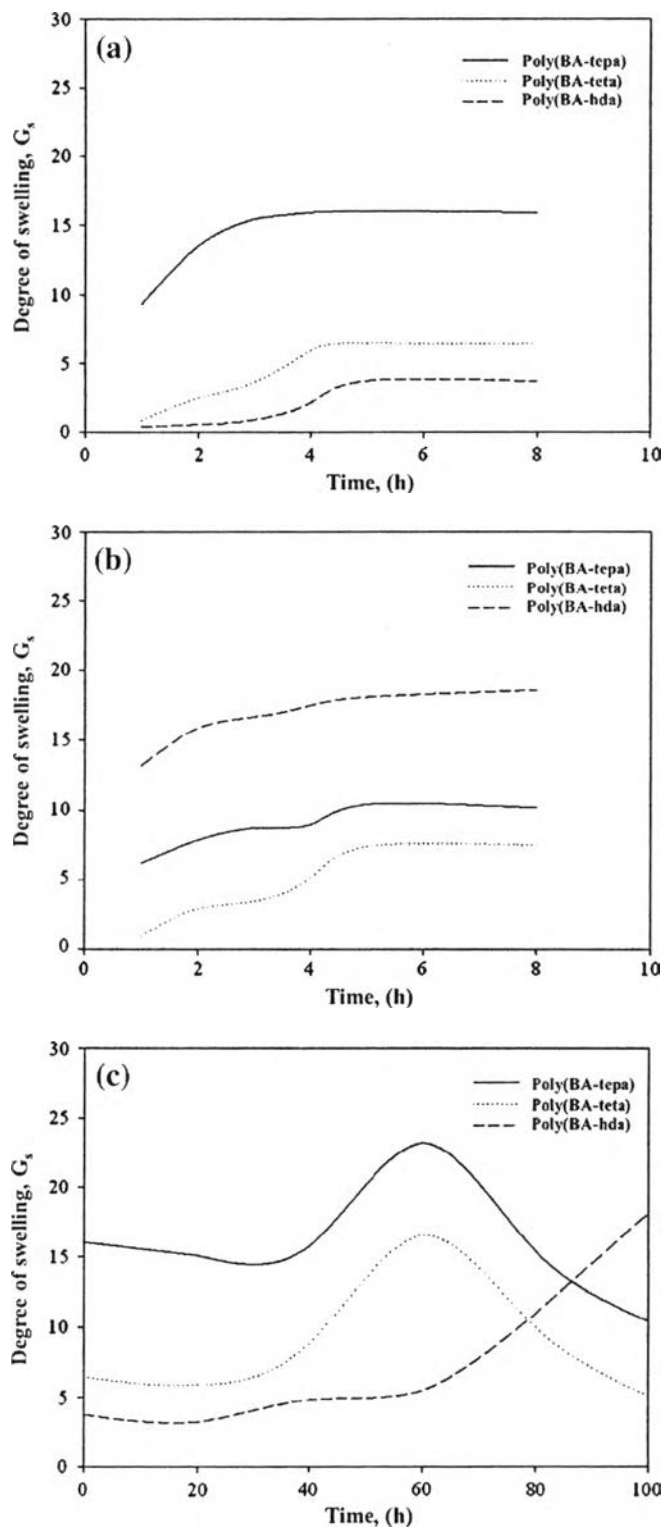


**Figure 4.5** Swelling degrees of polybenzoxazine membranes in water (a) and ethanol (b) with time, and in the ethanol–water mixtures (c).

ATR-IR was used to study the sorption behavior of the poly(BA-tepa) membrane using various ethanol–water concentrations (Figure 4.6). The characteristic peaks of ethanol and water were identified at  $2972\text{ cm}^{-1}$  and  $1639\text{ cm}^{-1}$ , respectively [21]. When the amount of ethanol was increased, the sorption of the poly(BA-tepa) membrane was also increased, as can be seen from the increased intensity of the characteristic peaks of ethanol. Likewise, the intensity of the characteristic peak of water decreased with the decrease of water concentration in the solution, indicating that both ethanol and water can penetrate the matrix of the poly(BA-tepa) membrane. Similar results were obtained when the poly(BA-teta) and poly(BA-hda) membranes were used. These results are in agreement with the study by Pereira et al. [22], where the sorption behavior of water and ethanol in a polymeric membrane using ATR-IR was reported. They found that the peak intensity of the water and ethanol sorption increased upon an increase in the water and ethanol concentrations.

#### 4.4.3. Pervaporation Analysis

According to the swelling and sorption results, the concentration of ethanol and water in the feed solution was an important factor in the stability of the polybenzoxazine membranes. The result of the swelling of poly(BA-hda) at high ethanol concentration showed a high degree of swelling, causing the membrane to be easily damaged during the pervaporation process, which was under vacuum pressure and slightly high temperature. In this study, the ratio between ethanol and water in the feed solution was kept at 1:9 because it was close to the alcohol concentration obtained from the fermentation process, which is approximately 12% by volume, and this ratio was suitable for our polybenzoxazine membranes according to the results of the sorption and the swelling. The feed temperature and the membrane thickness are also important parameters in the pervaporation process. The feed temperature was kept at  $70\text{ }^{\circ}\text{C}$ , while a thickness of  $200\text{ }\mu\text{m}$  was used to study the lifetime of each polybenzoxazine membrane. Figure 4.7 shows % ethanol in the retentate side, analyzed by GC, as a function of operating time. When compared to the membranes prepared from poly(BA-teta) and poly(BA-tepa), the one prepared from the poly(BA-hda) showed better physical integrity, even after 120 hours. This membrane could be

used for more than one week to separate the ethanol–water mixture. On the other hand, the service time for the poly(BA-teta) and poly(BA-tepa) membranes was approximately 12 and 3 hours, respectively. This might be due to the fact that poly(BA-hda) consists of long aliphatic chains in the structure, hence it was more flexible, whereas the poly(BA-tepa) and the poly(BA-teta) have nitrogen atoms in the structure, which could swell with water, thus leading to membrane damage [23]. The results also agreed with the results of the swelling behaviors mentioned above. Since the poly(BA-hda) membrane showed the best service time, it was chosen for further investigation.

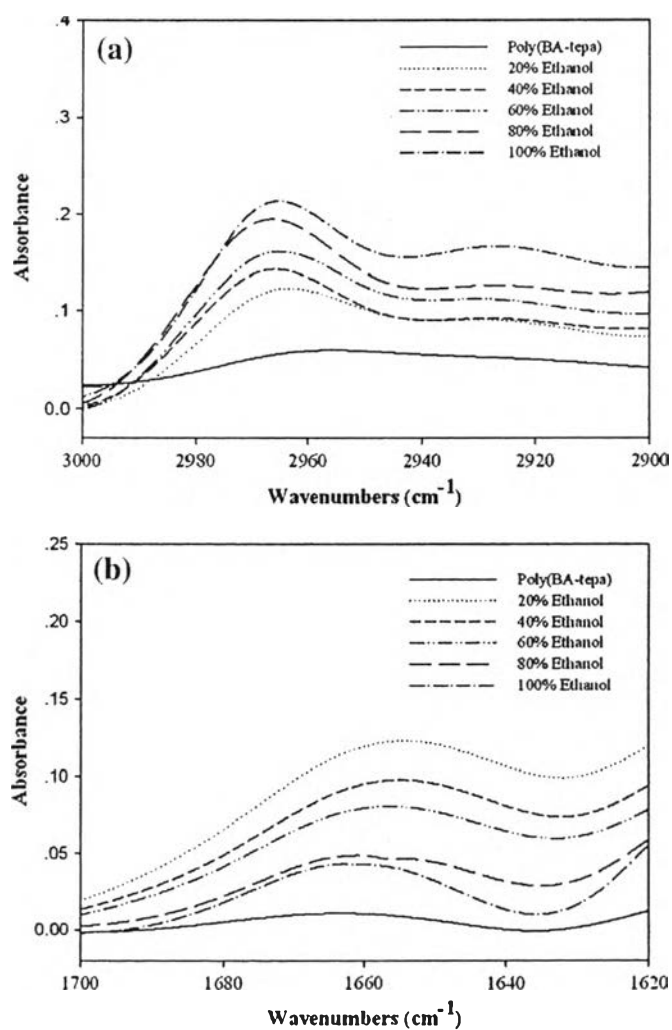


**Figure 4.6** ATR-IR spectra of the poly(BA-tepa) membrane immersed in the ethanol–water mixtures and the characteristic peaks of ethanol (a) and water (b).



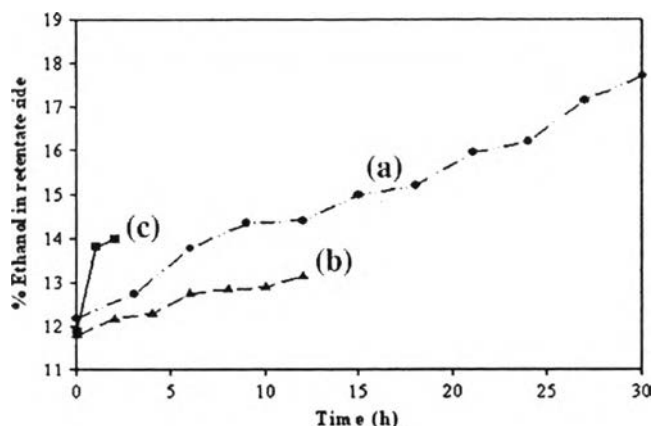


**Figure 4.7** % Ethanol in the retentate side of the poly(BA-hda) (a), poly(BA-teta) (b), and poly(BA-tepa) (c) membranes in the pervaporation process as a function of the operating time.

#### 4.4.3.1. Effect of Temperature

Figure 4.8 shows the permeate water flux of the pervaporation process using the poly(BA-hda) membrane as a function of operating temperature. The feed temperature was varied from 40, 50, 60, and 70 °C in the cell. Again, the feed solution was fixed at 1:9 for the ethanol–water ratio and the thickness of the poly(BA-hda) membrane was approximately 200 μm. The permeation flux was increased when the feed temperature was increased. At high temperature, the diffusion rate increased, leading to an enlarged permeation flux, as also reported by Huang Y. et al. [6]. In our study, only water molecules penetrated and moved across the poly(BA-hda) membrane, suggesting that the longer aliphatic chain length  $[-(\text{CH}_2)_6-]$  could absorb more ethanol, so it only allowed water molecules to pass through, resulting in a separation factor higher than 10,000 with the highest permeation flux of 1.52 kg/m<sup>2</sup>h at 70 °C. This temperature was later used to study the effect of the membrane thickness.

The activation energy of the pervaporation was obtained from the relationship between the temperature and the permeation flux, using the Arrhenius equation:

$$J = J_0 \exp\left(\frac{-E_p}{RT}\right) \quad (4.4)$$

Where  $J_0$  = permeation rate constant,  
 $E_p$  = activation energy for permeation,  
 $R$  = gas constant, and  
 $T$  = temperature (Kelvin, K).

From Figure 4.8, the apparent activation energy was a function of permeate concentrations, and the activation energy, calculated from the slope of the curve plotted between  $\ln J$  and  $1/T$ , was 3.74 kJ/mol.

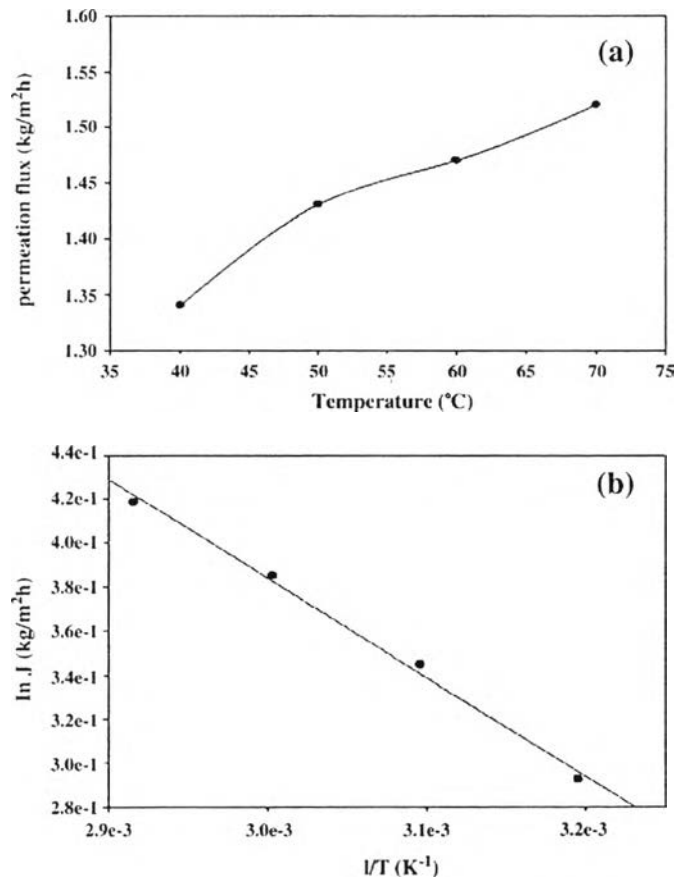


**Figure 4.8** Total permeation flux (a) and Arrhenius plot (b) of the poly(BA-hda) membrane in the pervaporation process as a function of the feed solution temperature.

#### 4.4.3.2. Effect of Membrane Thickness

Three different poly(BA-hda) membrane thicknesses were investigated (100, 200, and 300  $\mu\text{m}$ ). It is well-known that the permeation flux is proportional to the membrane thickness, and our results show similar trends. From Figure 4.9, the highest total permeation flux was found when the poly(BA-hda) with a thickness of 100  $\mu\text{m}$  was used. However, not only water but also ethanol molecules were found in the permeate side when permeate was analyzed using GC, resulting in a much lower separation factor (76.6) (Table 4.3). This might be due to the effect of swelling of the thin membrane, as also reported by Qunhui et al. [24], who studied the pervaporation separation of ethanol–water using a chitosan membrane; they found a decrease in the separation factor with decreasing membrane thickness. In our study, the separation factor of the 100  $\mu\text{m}$  thickness was rather low since about 0.2% by volume ethanol was found on the permeate side. On the other hand, only water was found on the permeate side when a membrane with a thickness of 200  $\mu\text{m}$  was used. This confirms that the thickness of the membrane indeed affects the separation performance of the membrane.

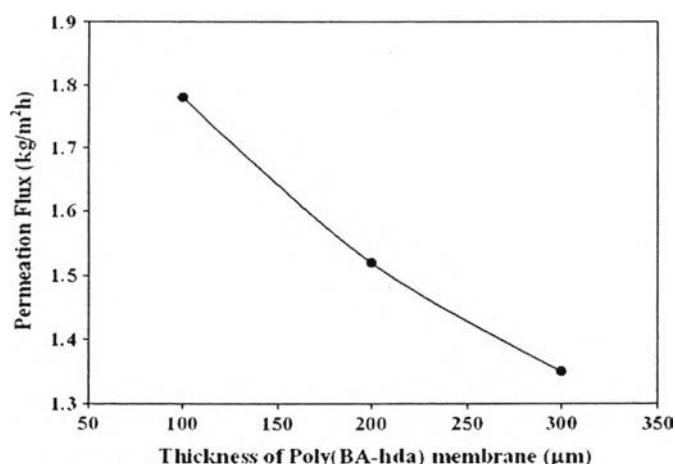


**Figure 4.9** Total permeation flux of the poly(BA-hda) membrane in the pervaporation process as a function of the membrane thickness.

**Table 4.3** Separation factors of the poly(BA-hda) membrane in the pervaporation process as a function of the membrane thickness.

Thickness of Poly(BA-hda) membrane ( $\mu\text{m}$ )	Separation factor ( $\alpha$ )
100	76.59
200	>10000
300	>10000

#### 4.4.4. Comparison of pervaporation performance

The performance of the polybenzoxazine membranes for ethanol–water separation using pervaporation, compared with those reported previously, is shown in Table 4.4. It is clear that the poly(BA-hda) membrane showed excellent separation performance when compared with other membranes under similar pervaporation conditions.

## 4.5 Conclusions

A number of polybenzoxazine membranes were examined for separating ethanol from an ethanol–water mixture with low ethanol concentration. The membrane derived from poly(BA-hda) showed the longest service time when compared with those prepared from poly(BA-teta) and poly(BA-tepa). The best temperature of the feed solution and the thickness of the poly(BA-hda) membrane for ethanol/water separation via the pervaporation process were 70 °C and 200  $\mu\text{m}$ , respectively. In fact, the total permeation flux of water through the 200  $\mu\text{m}$  thick poly(BA-hda) was 1.52  $\text{kg}/\text{m}^2\text{h}$  and its separation factor for the ethanol–water system was found to be higher than 10,000.

**Table 4.4** Performance of the polymer membranes in ethanol–water separation by pervaporation

Polymer membranes	Condition studied		Permeation flux(kg/m <sup>2</sup> h)	Separation factor( $\alpha$ )	References
	%Ethanol	Temperature(°C)			
BTDA/PDMS with ODA	10	87	0.5	1.5	[26]
BTDA/PDMS without ODA	10	88	0.3	2.4	[26]
BTDA/PDMS without ODA	10	20	0.2	7.5	[26]
6FDA/MDMS-MDMS	10	40	1.9	6.0	[27]
PMDA/MDMS-MDMS	10	40	0.56	10	[27]
PDMS	7	22	0.03	7.3	[28]
PDMS	0.3-3	30	0.52-0.90	3.1	[29]
Poly(BA-hda)	10	70	1.52	>10000	This study

#### 4.6 Acknowledgements

This research work is financially supported by The Petroleum and Petrochemical College; The National Center of Excellence for Petroleum, Petrochemicals, and Advanced Materials; the Ratchadapi-sake Sompote Endowment Fund, Chulalongkorn University; the Thailand Research Fund (TRF); the National Science and Technology Development Agency (NSTDA); and, the Development and Promotion of Science and Technology Talents project (DPST). Additionally, the authors would like to thank Mr. Robert Wright for the English copy editing.

#### 4.7 References

- [1] R.L.C.T. Paixao, L.J. Cardoso, M. Bettotti, *Fuel* 86 (2007) 1185.
- [2] M. Ameri, B. Ghobadian, I. Baratian, *Renewable Energy* 33 (2008) 1469.
- [3] C. Hailin, M. Radosz, B. Francis, S. Youqing, *Sep. Purif. Technol.* 55 (2007) 281.
- [4] M. Toraj, A. Aroujalian, A. Bakhshi, *Chem. Eng. Sci.* 60 (2005) 1875.
- [5] Y. Li, H. Zhou, G. Zhu, J. Liu, W. Yang, *J. Membr. Sci.* 297 (2007) 10.
- [6] Y. Huang, J. Fu, T. Pan, X. Huang, X. Tang, *Sep. Purif. Technol.* 66 (2009) 504.
- [7] H. Ahn, H. Lee, S.B. Lee, Y. Lee, *Desalination* 193 (2006) 244.
- [8] L. Fangfang, L. Li, F. Xianshe, *Sep. Purif. Technol.* 42 (2005) 273.
- [9] X. Ning, H. Ishida, *J. Polym. Sci.* 32 (1994) 1121.
- [10] T. Takeichi, T. Kano, T. Agag, *Polymer* 46 (2005) 12172.
- [11] T. Agag, T. Takeichi, *J. Polym. Sci. Part A: Polym. Chem.* 45 (2007) 1878.
- [12] D.J. Allen, H. Ishida, *J. Appl. Polym. Sci. Part B: Polym. Phys.* 101 (2006) 2798.
- [13] K. Hajime, M. Akihiro, H. Kichi, F. Akinori, *J. Appl. Polym. Sci.* 72 (1999) 1551.
- [14] K. Hajime, T. Shuuichi, M. Akihiro, *J. Appl. Polym. Sci.* 79 (2001) 2331.
- [15] P. Lorjai, T. Chaisuwan, S. Wongkasemjit, *J. Sol-Gel Sci. Technol.* 52 (2009) 56.

- [16] P. Lorjai, T. Chaisuwan, S. Wongkasemjit, *Mater. Sci. Eng., A* 527 (2009) 77.
- [17] T. Takeichi, T. Agag, *High Perform. Polym.* 18 (2006) 777.
- [18] J.R. Gonziilez-Velasco, J.A. Gonzilez-Marcos, C. Lbpez-Dehesa, *Desalination* 149 (2002) 61.
- [19] D. Vesely, *Polymer* 42 (2001) 4417.
- [20] W.Y. Chuang, T.H. Young, D.M. Wang, R.L. Luoc, Y.M. Sunc, *Polymer* 41 (2000) 8339.
- [21] D. Murphy, M.N. de Pinho, *J. Membr. Sci.* 106 (1995) 245.
- [22] A.M.M. Pereira, M.C. Lopes, J.M.K. Timmer, J.T.F. Keurentjes, *J. Membr. Sci.* 260 (2005) 174.
- [23] H.D. Kim, H. Ishida, *J. Appl. Polym. Sci.* 79 (2001) 1207.
- [24] G. Qunhui, H. Ohya, Y. Negishi, *J. Membr. Sci.* 98 (1995) 223.
- [25] J.Y. Lai, S.H. Li, K.R. Lee, *J. Membr. Sci.* 93 (1994) 273.
- [26] M. Krea, D. Roizard, N. Moulai-Mostefa, D. Sacco, *J. Membr. Sci.* 241 (2004) 55.
- [27] Y. Huang, L.M. Vane, *BioSep™: a new ethanol recovery technology for small scale rural production of ethanol from biomass*, AICHE, San Francisco, CA, November, (2006).
- [28] T. Mohammadi, A. Aroujalian, A. Bakhshi, *Chem. Eng. Sci.* 60 (2005) 1875.